Available online at www.sciencedirect.com
SCIENCE DIRECT®
PERGAMON
Minerals Engineering 16 (2003) 135–144
MINERALS ENGINEERING
This article is also available online at: www.elsevier.com/locate/mineng

Interference of coarse and fine particles of different shape in mixed porous beds and filter cakes ☆

M. Mota [a,*], J.A. Teixeira [a], W.R. Bowen [b], A. Yelshin [a]

[a] *Centro de Engenharia, Biologica—IBQF, Universidade do Minho, Braga 4710-057, Portugal*

[b] *Centre for Complex Fluids Processing, University of Wales, Swansea, UK*

Received 18 June 2002; accepted 7 November 2002

Abstract

In solid–liquid separation the knowledge of solids packing structure is important to control permeability and dewaterability. In particular, cakes formed in filtration are often represented by the composition in coarse and fine particles. In this work cakes were modelled by mixing a bed of coarse (spheres) and fine (kieselguhr of three types and kieselgel) particles with a wide size distribution, in order to obtain beds with different proportions of plate and rod-like particles. Size ratio of glass beads to kieselguhr particles were in the range 23–30. Porosity and permeability were measured for a range of large particle fraction in the mixture from 0 up to 1.0. The fractional porosity of each particle fraction was introduced as a parameter. The approach proposed in this work was also successfully applied to different published filtration data. It was found that (1) the presence of more than 10% of fines in the coarse granular bed significantly reduces the cake permeability; (2) to improve cake permeability the volume fraction of filter aid in suspension must be at least 50–60% of total solid volume; (3) obtained data may be used to control the porosity of a mixture, if the fractional porosity of large and small particles is known or to estimate mixture tortuosity.

Keywords: Dewatering; Filtration

1. Introduction

Mixtures of irregular and regular (close to sphere) particles are widely used in practice. In solid–liquid separation we often have suspensions where solids can be clearly separated in two particle fractions of significantly different size (large: coarse, small: fine).

Perlite and kieselguhr are used as filter media and filter aids for filtration of suspensions of different nature (Weismantel, 2001; Weler, 1972; Yoon et al., 1992; Rushton et al., 1996). Simultaneously, kieselguhr filter aids, represented by highly irregular particles, may represent an excellent experimental model for the investigation of the behaviour of mixtures of irregular particles with regular (granular) material. Numerous filter cakes and sediments represent such type of binary mixtures. Binary mixtures of two particle types, irregular and granular were investigated in this work. Depending on conditions, granular particles represent fraction of large size D or small size d particles and irregular particles play the role of the other mixture's fraction.

Tiller et al. (1988a,b) investigated the effect of filter aids on optimum filter cycle in batch filtration and pointed out that, in contrast to the usual assumption that there is a fixed fraction of filter aid admix which yields the best results, the optimum amount of filter aid may vary with cake thickness, washing and dead time.

The relationship between bed porosity of non-spherical particles and the particle sphericity factor was discussed by Yu et al. (1996) for particles of defined geometry: cylinder, sphere, disc. However, the behaviour of mixtures in real systems such as filter cakes, sediments, etc. needs to be compared with those with a defined geometrical packing. Klusácek and Schneider (1981) investigated the effect of size and shape of catalyst microparticles on pellet pore structure and its effectiveness

☆ Presented at *Solid–Liquid Separation '02* Falmouth, UK, June 2002.

* Corresponding author. Tel.: +351-253-604405; fax: +351-253-678986.

E-mail address: mmota@deb.uminho.pt (M. Mota).

0892-6875/03/$ - see front matter © 2003 Elsevier Science Ltd. All rights reserved
doi:10.1016/S0892-6875(02)00314-X

Nomenclature

a, b, c and n	coefficients	ε_D	particular porosity of large size particle fraction
D	average diameter of large particles, m	ε_d	particular porosity of small size particle fraction
d	average diameter of small particles, m	ε_D^0	porosity of the large particles bed
v_D	glass beads volume in the mixture, m^3	ε_d^0	porosity of the small particles bed
v_d	irregular particles volume in the mixture, m^3	$\varepsilon_{\min}$	minimum porosity
x_D	volume fraction of large particles in the total volume of particles in the mixture	Φ	shape factor
$\delta = d/D$	size ratio of small to large particles		
ε	overall porosity of the mixed bed		

using as binary mixtures ion exchange resin particles with glass beads, crushed glass or glass slabs. Each mixture was represented by a limited number of samples with a defined particle size ratio and different proportions of small and large particles which make it difficult to draw generalised conclusions.

Measured porosities were presented by Abe and Hirosue (1982) for filter cakes with a mixture of filter aid "Filter-Cel" and kaolin. Later Okoh (1989) investigated porosity and specific cake resistance as a function of volume fraction of different filter aids. These authors observed that a proportion 10% or less of filter aid in the suspension gives rise to a low porosity. It is therefore clear that information about overall porosity does not suffice to predict the filtration behaviour of mixtures.

In the above-mentioned works the large size particle fraction was kieselguhr. In turn, the situation when the large size particle fraction is composed of spheres, as was used by Mota et al. (1998), has been less investigated. However, this type of mixture can give useful information about the behaviour of non-spherical large particles when, for example in slurry filtration on belt and pan filters or in compacted clay with granular inclusions (Meeten and Sherwood, 1994).

The fractional porosity approach (Mota et al., 2001) allows for a better understanding of the influence of each particle fraction in a binary mixture. As experimental model a mixture of spherical particles (glass beads) and small size kieselguhr particles was chosen. Our experimental results, together with other published data, were then used to develop a generalised approach to explain the porous media properties based on fractional porosity.

2. Materials and methods

Three types of the kieselguhr and kieselgel, mixed with spherical glass beads of mean size $D = 337.5 \times 10^{-6}$ m were investigated. In mixtures with glass beads, the particle size ratio D/d was as follows: kieselgel—23.3; kieselguhr-G—27.4; kieselguhr middle size—29; kieselguhr fine—27.5. Middle and fine kieselguhrs were samples of commercially used kieselguhrs. Glass beads

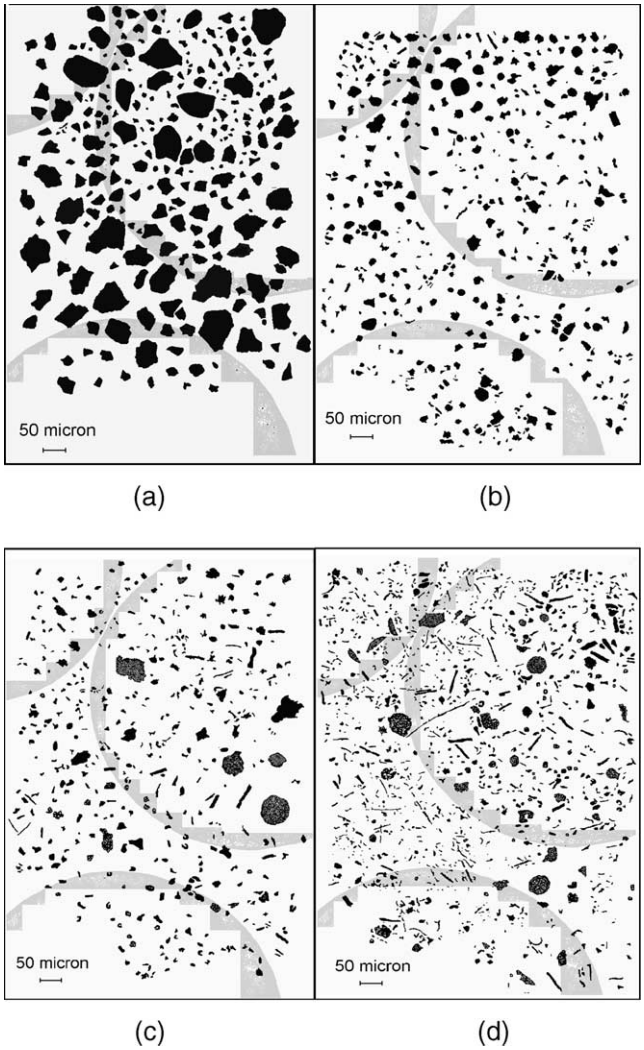

Fig. 1. View of kieselgel and kieselguhrs particles used in binary mixtures preparation. To compare sizes the border of glass beads is shown as a grey shadow contour: (a) kieselgel, (b) kieselguhr-G, (c) kieselguhr of middle size and (d) kieselguhr fine.

were the largest particles in the mixture and their volume fraction in the mixture was defined as x_D.

Particle shape was defined using image analysis. All samples contain plate and rod irregular particles, and disc-like particles were also observed in kieselguhrs (Fig. 1). Particle size distribution was measured by means of particle size analysing system GALAI-CSI-100 with computerised inspection system. Two samples of each kieselguhr were analysed. Distribution of the average probability on particle size d is shown in Fig. 2 together with results of multiple Gaussian analysis application.

Particles are shown in Fig. 1, where a procedure of grey map filter (linear filter) was applied. As term of comparison a border of glass beads is shown as grey background. All particles in the micrograph are viewed in a plane projection.

Each mixed bed of irregular particles and glass beads was formed in a cylindrical filter unit (diameter 32 mm) and then saturated by water. Before measuring porosity and permeability and in order to stabilise the bed 1000 ml of distilled water were passed through the bed. The applied filtration pressure was 40 kPa. For qualitative analysis filter-paper type MN-763, Macherey-Nagel GmbH & Co., was used as the layer support. Glass beads served as large size particle fraction and their volume fraction in the mixture was defined as $x_D = v_D/(v_D + v_d)$, where v_D is a volume of glass bead particle in the mixture and v_d is a volume of irregular (small) particles in the mixture. The mixed bed porosity was measured before and after the filtration experiments. Porosity was determined by measuring the total volume of the mixture in the cylinder and the volume of water used to fill in completely the porous medium.

3. Results and discussion

3.1. Kieselguhr fractional content

The results of particle size distribution in the fraction of fine particles are shown in Fig. 2. As seen in this figure, kieselguhrs and kieselgel have complex fractional composition represented by three and even four (kieselguhr fine) overlapped sub-fractions. The experimental curves become more complex as we move from kieselgel to kieselguhr fine. In Fig. 2, for comparison, log-normal simulated curves are shown based on mean particle size as it was measured in experiment.

The effect of irregular particle shape on the overall mixture porosity may be estimated using a shape factor Φ. Below we use the shape factor, as it was given by Yu et al. (1996), in the form of an empirical equation for dense $\ln(\varepsilon_d^0) = \Phi^{6.74}\exp[8(1-\Phi)]\ln(0.36)$ and loose $\ln(\varepsilon_d^0) = \Phi^{5.58}\exp[5.89(1-\Phi)]\ln(0.40)$ random packing of cylinders: Curves obtained by Brownell et al. (1950) for irregular monosize particle packing, are also shown in Fig. 3. In our case a parameter ε_d^0 corresponds to the porosity of pure kieselguhr or kieselgel bed.

As may be seen, only the shape factor of middle size kieselguhr fits with the model of dense packing of cylinders.

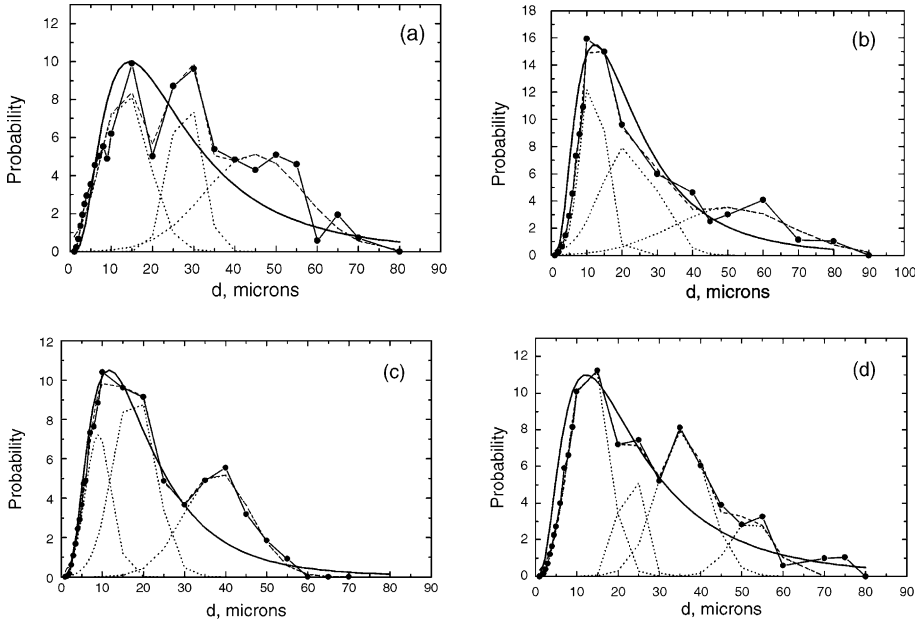

Fig. 2. Particle size distribution measurements (points with solid line), obtained from multiple Gaussian analyses: dashed line—fitting function; dotted peaks—fractions distribution; and simulated log-normal distribution (solid curve). (a) Kieselgel, (b) kieselguhr-G, (c) kieselguhr of middle size and (d) kieselguhr fine.

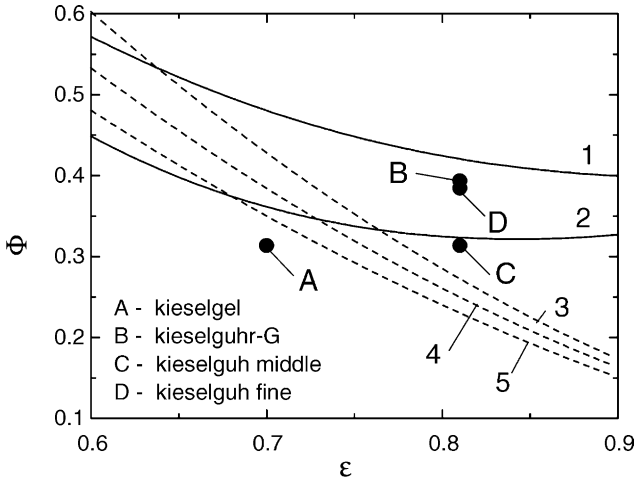

Fig. 3. Comparison of the shape factors Φ of kieselgel and kieselguhrs determined by image analysis with the ones calculated for loose (curve 1) and dense (curve 2) packing of cylinders by Yu et al. (1996). Curves 3–5 represent loose (curve 3), normal (curve 4), and dense (curve 5) packings of irregular particles obtained by Brownell et al. (1950).

3.2. Porosity, theoretical approach

Although a model of irregular particle mixture becomes complex when particle size distribution occurs (Yu and Standish, 1991, 1993; Yu et al., 1993, 1996), as is our case, when components can be separated in two fractions (glass beads and kieselguhr), it is possible to apply a binary mixture model (Mota et al., 1999, 2000, 2001). With this approach it is possible to analyse the influence of each particle fraction on the overall porosity in all range of x_D by means of a fractional porosity approach.

Let us represent the overall porosity ε as a function of fractional porosity $\varepsilon_D = \varepsilon_D(x_D)$ and $\varepsilon_d = \varepsilon_d(x_D)$, where ε_D is the void fraction of large particles in the total volume of the mixture, and ε_d is the specific void fraction of small particles in the remaining void volume of the mixture. Since the overall volume of solids in the mixture, $1-\varepsilon$, is a sum of volumes of large particles, $1-\varepsilon_D$, and small particles, $(1-\varepsilon_d)\varepsilon_D$, the porosity of the mixture becomes (Mota et al., 2000),

$$\varepsilon = \varepsilon_D \varepsilon_d \tag{1}$$

3.2.1. Fractional porosity of fine particles, ε_d

In mixtures enriched with fine particles, the coarse particles are evenly distributed within the small particles matrix. When the particle size ratio D/d is large, if the inter-fractional interaction is neglected, a constant porosity ε_d for the fine particles is expectable, hence, $\varepsilon_d \approx \varepsilon_d^0 = \text{const}$, where ε_d^0 is the porosity of the bed of pure fine particles. This condition is characterised by the line *abc* in Fig. 4a.

For mixtures enriched with large particles the amount of fine particles becomes insufficient to fill all free space between large particles skeleton and ε_d increases linearly, as represented by lines *bd* or *cd* (depending on the fine particles arrangement in the skeleton, Fig. 4b) up to $\varepsilon_d = 1.0$. We consider two possible fine particles arrangements: (a) filling the void between large particles and (b) intrusion of fine particles in the large particles skeleton. In this case the dependence of ε_d vs. x_D may be represented by linear function $\varepsilon_d = ax_D + b$ with coefficients a and b, $a + b = 1.0$. Therefore the function ε_d contains two parts: constant, ($\varepsilon_d \approx \varepsilon_d^0$) and linear.

3.2.2. Fractional porosity of coarse particles, ε_D

By representing the volume fraction of fine particles in the mixture as $v_d = \varepsilon_D(1-\varepsilon_d^0)$ the volume fraction of the large particles in the mixture may be written as

$$x_D = \frac{v_D}{v_D + v_d} = \frac{1-\varepsilon_D}{1-\varepsilon_D\varepsilon_d^0} \tag{2}$$

and we obtain large particles fractional porosity in the form

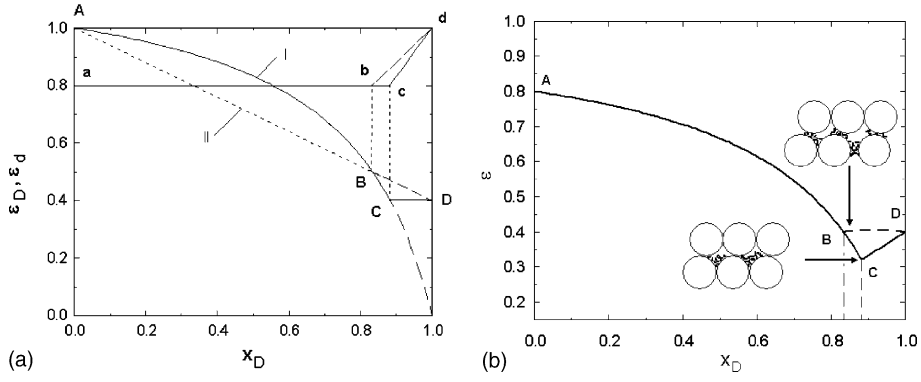

Fig. 4. Theoretical dependences of the fractional porosity ε_D and ε_d (a) and overall porosity ε (b) on x_D. (a) Lines *abcd* or *abd* are the dependence of ε_d on x_D. Curve I: Eq. (3), curve II: Eq. (4). (b) Curve *ABD* generated by the segment *AB*, Eq. (5), and segment *BD*, Eq. (6a). Curve *ACD*: segment *AC*, Eq. (5), and segment *CD* Eq. (6b). The following initial conditions were assumed: $\varepsilon_D^0 = 0.4$ and $\varepsilon_d^0 = 0.8$. Points *B* and *C* correspond to $x_D = 0.833$ and 0.881, respectively.

$$\varepsilon_D = (1 - x_D)/(1 - x_D\varepsilon_d^0) \quad (3)$$

which is shown in Fig. 4a as a curve (I).

The right-hand branch of ε_D for mixtures enriched with large (coarse) particles may be defined through boundary conditions. The first boundary is represented by the segment *BD* of the dependence (4) (Fig. 4a, line (II)). Eq. (4) corresponds to a "linear" mechanism of large particles packing that in our case is similar to fine particle intrusion into skeleton of coarse fraction:

$$\varepsilon_D = 1 - (1 - \varepsilon_D^0)x_D \quad (4)$$

The second boundary corresponds to the condition $\varepsilon_D \approx \varepsilon_D^0 = \text{const}$, where ε_D^0 is the porosity of the bed of pure coarse particles: segment *CD*. In this case we have the large particles skeleton with fine particle fraction fully distributed inside the skeleton void.

3.2.3. Overall mixture porosity ε

In Fig. 4b the overall porosity, a product of fractional porosities, is shown with the following initial conditions: $\varepsilon_D^0 = 0.4$, the usual glass beads packing porosity and $\varepsilon_d^0 = 0.8$, which is close to the kieselguhr packing porosity. Points *B* and *C* correspond to $x_D = 0.833$ and 0.881, respectively.

In mixtures enriched with fine particles, when $\varepsilon_d = \varepsilon_d^0$, the overall porosity is, according to Eq. (3),

$$\varepsilon = \varepsilon_D\varepsilon_d^0 = \frac{(1 - x_D)\varepsilon_d^0}{1 - x_D\varepsilon_d^0} \quad (5)$$

Eq. (5) theoretically describes the left-hand part of the dependence ε on x_D (Fig. 4b) and is represented by the curved segment *AB* or *ABC* depending on the boundary conditions mentioned above. Therefore, ε in the case of mixtures with coarse particles will be defined, according to Eq. (1), by the following equations

$$\varepsilon = (1 - (1 - \varepsilon_D^0)x_D)\varepsilon_d \quad (6a)$$

or

$$\varepsilon = \varepsilon_D^0\varepsilon_d \quad (6b)$$

where ε_d is some function, in particular $\varepsilon_d = ax_D + b$.

3.3. Experimental porosity, ε

Experimental overall porosity obtained for binary mixtures is shown in Fig. 5. A curve similar to the theoretical type ABCD (see Fig. 4) was observed for kieselgel and kieselguhr-G; a curve of the theoretical type *ABD* was obtained for kieselguhr fine and middle. The overall porosity has minimum values of x_D around 0.9. The curve *ABCD* may be due to the fact that kieselgel and kieselguhr-G fill the void between large particles; in turn, the curve *ABD* may be explained by the intrusion of fine particles in the skeleton built by the large particles. Probably this difference of packing mechanism is due to a different particle shape distribution. Kieselguhrs middle and fine have a wider particle shape variety as compared with kieselgel and kieselguhr-G (see Fig. 1).

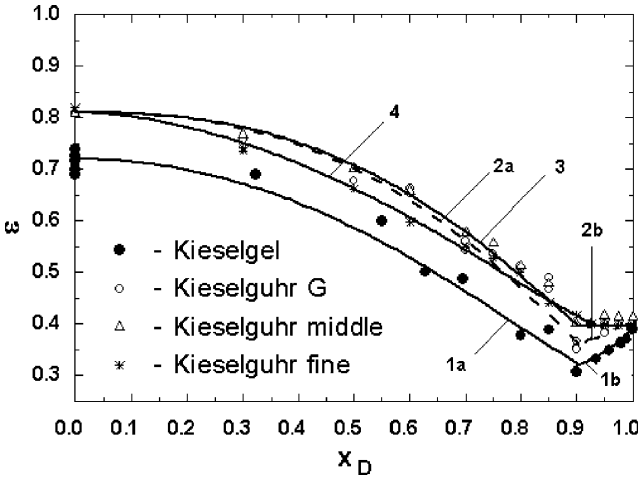

Fig. 5. Experimental dependence of mixed bed porosity ε on volume fraction of large particles (glass beads) x_D (points) and obtained correlation functions presented in Table 1. Curves 1a and 2a: fitting functions for kieselgel; curves 2a and 2b: kieselguhr-G; curves 3 and 4: kieselguhr of middle and fine size, respectively.

The results on experimental dependence of ε on x_D show some similarity with the results presented in the work of Yu et al. (1996) (see Fig. 9) but the particle size ratio values in our case are 2–3 times higher. For example, a transition of the right-hand part of the dependence from a horizontal to an inclined trend in Yu et al. (1996) corresponds to $d/D \sim 0.1$ whereas this transition in our case is for d/D is in the range 0.03–0.043.

3.3.1. Experimental fractional porosities and their correlation functions

The particle interaction, on the one hand, and the particle size distribution, on the other hand, gives rise to a deviation from theoretical approach as defined by Eq. (3). This deviation may be seen in detail if, instead of the overall porosity ε, the binary mixture porosity is expressed in terms of fractional porosities (Fig. 6).

Dependencies ε_D and ε_d on x_D in Fig. 6 are built on the experimental data points. It follows from Fig. 6 that the porosity, $\varepsilon_d(x_D)$ in the range of $x_D < 0.8$, may be assumed to be constant and equal to ε_d^0 as the theoretical model predicts. However, in the range of $0.9 > x_D > 0.8$ the fine particles fractional porosity changes smoothly from $\varepsilon_d = \varepsilon_d^0$ to $\varepsilon_d = ax_D + b$. This observation leads to the conclusion that the observed transition is due to the simultaneous action of both packing mechanisms: filling the skeleton void volume on the one hand and intrusion into the skeleton of fine particles, on the other.

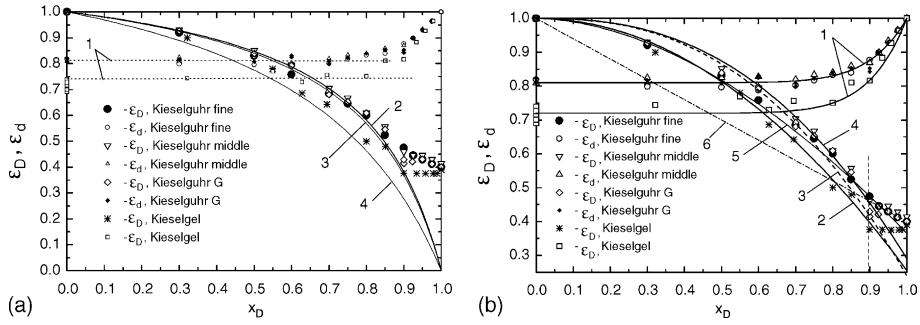

Fig. 6. Dependence of ε_D and ε_d on the volume fraction of large particle in mixtures x_D. (a) Theoretical model: curve 1—$\varepsilon_d = \varepsilon_d^0 = \text{const}$; solid curves 2–4 is ε_d^0 by Eq. (3); 2—$\varepsilon_d^0 = 0.82$, 3—$\varepsilon_d^0 = 0.8$, and 4—$\varepsilon_d^0 = 0.71$. (b) The correlation functions for fitting experimental data: 1—$\varepsilon_d(x_D)$, Eq. (9); 2–5: fitting functions of $\varepsilon_D(x_D)$ (see Table 1), where 2—kieselgel; 3—kieselguhr-G; 4—kieselguhr of middle size, and 5—kieselguhr of fine size. 6—line $\varepsilon_D = (1 - 0.6x_D)$, Eq. (4).

Moreover, around $x_D = 0.9$, Kieselguhr of middle and fine sizes with rod-like particles the dependence $\varepsilon_D(x_D)$ follow Eq. (4) (Fig. 6b, line 6), whereas kieselgel and kieselguhr-G with plate-like particles follow the condition $\varepsilon_D = \varepsilon_D^0 = \text{const}$.

In the range of minimum porosity, the following relations were applied (Mota et al., 2001):

$$\varepsilon_d(x_D) = \varepsilon_d^0 + (1 - \varepsilon_d^0)x_D^{f(\delta)} \tag{7}$$

$$\varepsilon_D(x_D) = 1 - (1 - \varepsilon_D^0)x_D^F \tag{8}$$

where power indexes $f(\delta)$ and F are correction functions depending on the ratio δ. Correlation functions for mixtures of kieselguhr–glass beads were evaluated. As the δ values in the investigated mixtures have a narrow dispersion, we may assume in Eq. (7) that $f(\delta) = \text{const}$ and, from fitting analysis, to be equal to 10 (see Fig. 6b, curves 1):

$$\varepsilon_d(x_D) = \varepsilon_d^0 + (1 - \varepsilon_d^0)x_D^{10} \tag{9}$$

The advantage of relation (9), as compared with the theoretical *abd* or *acd* lines (Fig. 4a) is that we may work with a continuous function.

The significant deviation of small particles shape from spherical particle shape did not allow us to adopt Eq. (8) directly for non-spherical particles in all range of x_D and a fitting procedure was applied. Dependence $\varepsilon_D(x_D)$ was divided in two parts: part 1 corresponds to the range of x_D from zero up to the point of minimum porosity, $x_{D\min}$, and part 2 goes from $x_{D\min}$ up to 1.0.

Part 1 of the dependence corresponds to Eq. (10) and keeps the form of relation (8) except for a value of coefficient c that was not equal $(1 - \varepsilon_D^0)$:

$$\varepsilon_D(x_D) = 1 - cx_D^n \tag{10}$$

where c and n is the constant, and part 2 of the dependence for kieselgel and kieselguhr-G was as theoretical (6b): $\varepsilon_D^0\varepsilon_d(x_D)$, and for kieselguhr of middle and fine size as (6a): $(1 - 0.6x_D)\varepsilon_d(x_D)$, where ε_D^0 is the porosity of the pure glass bead packing. All the obtained correlation functions for overall porosity are given in Table 1, and shown in Fig. 5.

3.4. Permeability

The permeability k of mixed beds was measured as described in Mota et al. (2001) and are shown in Fig. 7. As can be seen, the minimum permeability value does not coincide with minimum porosity. This is the result of the effect on permeability of parameters such as pore tortuosity and average pore size, both dependent on x_D. However, it is clear that the minimum permeability corresponds to the transition region of the fine particles fractional porosity, ε_d, in the range of x_D between 0.7 and 0.9.

The mixture permeability increases for $x_D \geqslant 0.9$ and may also be modelled using Eq. (1) and a tortuosity function, as described by Mota et al. (2001).

Table 1
Correlation functions for experimental porosity $\varepsilon = \varepsilon_d\varepsilon_D$ vs. x_D

Material	Fitting function	
	$x_D = 0/x_{D\min}$	$x_D = x_{D\min}/1.0$
Kieselgel	$\varepsilon = (0.72 + 0.28x_D^{10})(1 - 0.745x_D^2)$	$\varepsilon = 0.39(0.72 + 0.28x_D^{10})$
Kieselguhr-G	$\varepsilon = (0.81 + 0.19x_D^{10})(1 - 0.76x_D^{2.5})$	$\varepsilon = 0.41(0.81 + 0.19x_D^{10})$
Kieselguhr middle	$\varepsilon = (0.81 + 0.19x_D^{10})(1 - 0.71x_D^{2.5})$	$\varepsilon = (0.81 + 0.19x_D^{10})(1 - 0.6x_D)$
Kieselguhr fine	$\varepsilon = (0.81 + 0.19x_D^{10})(1 - 0.635x_D^{1.8})$	
Bentonite + barite filter cake (Meeten and Sherwood, 1994)	$\varepsilon = (0.887 + 0.113x_D^{15})(1 - 0.8x_D^3)$	$\varepsilon = 0.385(0.887 + 0.113x_D^{15})$

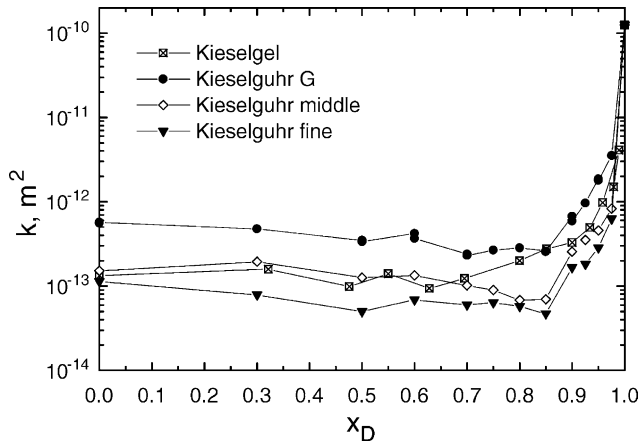

Fig. 7. Experimental dependence of the mixed beds permeability k on volume fraction of large particles, x_D, in the mixtures.

Finally, we must check whether the fractional porosity approach is sufficiently close to those data obtained experimentally by other authors.

3.5. Fractional porosity representation for filter cake and other binary packings

The porosity approach may be extended to other binary systems. The following data on binary systems were collected from publications referred below: (1) cakes : bentonite + barite (Meeten and Sherwood, 1994); TiO_2 + perlite, $CaCO_3$ + talc, liquefied coal residue + celite (Okoh, 1989); (2) Packing: Binary mixtures of cubes or spheres, mixtures of disks, binary mixtures of short and long cylinders, binary mixtures of sphere and cylinders (Yu et al., 1993, 1996).

3.5.1. Cake and binary packings of large granular (regular) and fine irregular particles

Meeten and Sherwood (1994) investigated the hydraulic permeability of bentonite suspensions (95% of particles of a size under 5 μm) with granular inclusions (barite, particle size 40 μm). Compacted clays were made by filtering aqueous suspensions of bentonite with barite, which formed granular inclusions in the filter cake.

Because of the large particle size ratio and of the presence in the binary mixture of granular (large size fraction) and plate-like bentonite particles it is reasonable to expect a behaviour similar to the one found in glass beads–kieselguhr mixtures. Meeten and Sherwood (1994) data were recalculated in the following manner: the large particle volume fraction was calculated as $x_D=\phi_b/(\phi_b+\phi_c)$, the overall porosity by $\varepsilon=e/(1+e)$, the particular porosity by $\varepsilon_D=1-\phi_{bc}$ and $\varepsilon_d=\varepsilon/\varepsilon_D$, where $\phi_c=0.02473$ is the bentonite volume fraction, e is the void/solid volumes ratio in the cake, and ϕ_{bc} is the volume fraction of barite in the cake. Obtained results and model equations are presented in Fig. 8A and Table 1, respectively.

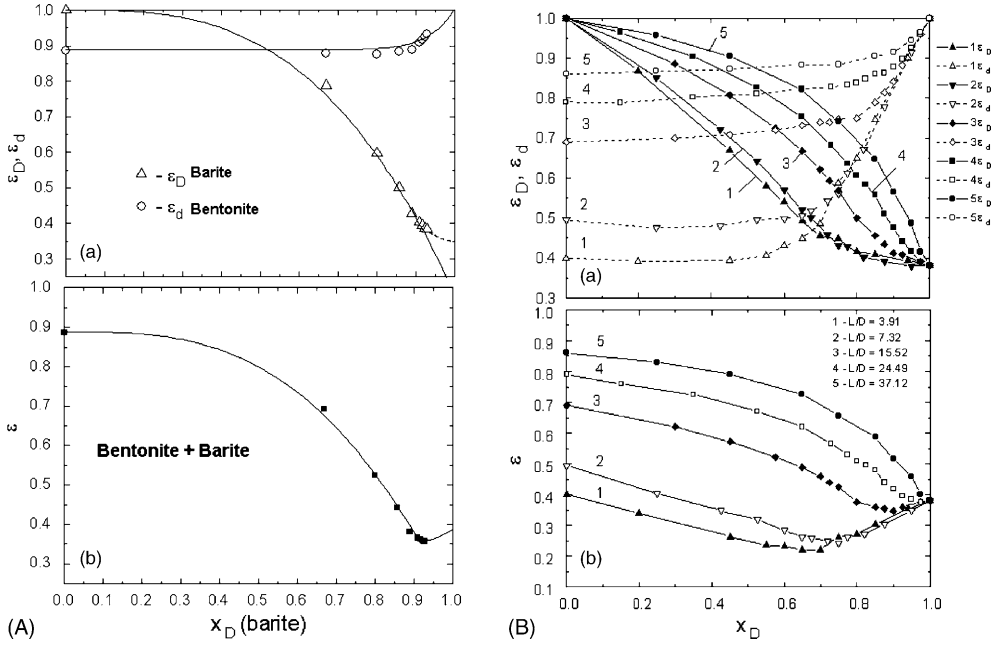

Fig. 8. Fractional (a) and overall porosity (b) diagrams vs. x_D for the bentonite + barite filter cake (A) and (B) sphere + cylinder packing. (A) Data of Meeten and Sherwood (1994) for the filter cake of bentonite + barite: (a) ε_D is the porosity of barite (dashed segment: extrapolation to ε_D^0) and ε_d the bentonite, (b) fitting functions (see Table 1). (B) Binary mixtures of sphere and cylinders of different dimensionless length L when the diameter D ratio of sphere to cylinder is 17.4. Fractional porosities obtained from data by Yu et al. (1996) for overall porosity. Fractional and overall porosities have the same symbols whereas open and solid symbols in (a) belong to ε_D and ε_d, respectively (L/D: curve 1—3.91; curve 2—7.32; curve 3—15.52; curve 4—24.49; and curve 5—37.12).

For a volume fraction x_D of barite up to about 0.9 the filter cake permeability is largely determined by the permeability of the interstitial bentonite–water matrix. The fractional porosity diagram and the permeability dependence observed by Meeten and Sherwood (1994) are similar to those obtained for the glass beads + kieselguhr.

It is more interesting to observe how the small particles shape affects the overall porosity. When spheres represent the large size particle fraction Yu et al. (1996) obtained a dependence of ε vs. x_D for the mixture of spheres and cylinders as displayed in Fig. 8B. We used the equations $x_D = \phi_D/(\phi_D + \phi_d) = (1-\varepsilon_D)/(1-\varepsilon)$, hence $\varepsilon_D = 1 - x_D(1-\varepsilon)$, and $\varepsilon_d = \varepsilon/\varepsilon_D$.

Fig. 8B clearly shows significant changes of the overall and fractional porosities. First of all we may see that the behaviour of ε_d is similar to the observed for the above-discussed binary systems. However, when the length of the cylinder increases (increasing the deviation from the granule shape) the influence of small particles on large particle fractional porosity ε_D becomes more important.

For a small and moderate ratio $L/D < 7$, both ε and ε_D, ε_d behave as spheres of different size packing (Mota et al., 2001). For $L/D > 7 - 10$ a significant increase of ε_d^0 takes place and the small size particles effect on the overall porosity is greater. Mixtures 3 and 4 (Fig. 8B) show similarity with kieselguhr–glass beads system whereas for mixture 5 the effect of extremely long cylinders is observed across all range of x_D.

3.5.2. Mixtures of particles of different irregularity

Let us now consider the fractional porosity of mixtures with particles of different types of irregularity.

The fractional porosity is useful also for systems where the particle size ratio is small. In Fig. 9A we present a fractional porosity diagram (a) obtained from overall porosity of mixtures of large and small cubes as well as of large cubes and spheres based on data of Yu et al. (1993). In this system, when the size ratio does not exceed 4, the large particles fractional porosity follows the linear model (Fig. 4a, line II), except for case (3), and the interaction of both fractions is significant in the whole range of x_D (Fig. 9A: a).

For case (3) we must point out an important detail: the fractional porosity allows detecting miscalculation or error in measure of the overall porosity and, in particular, to estimate the position on minimum porosity $\varepsilon_{\min}$ in graph (b). When we look at ε_d and ε_D vs. x_D then the points position corresponding to $\varepsilon_{\min}$ seems smaller than general trends (possibly due to error in measure of ε) and, therefore, if ε_d and ε_D were corrected to the trends their values would increase and $\varepsilon_{\min}$ point would move up smoothing the relation ε vs. x_D.

Other examples may be obtained from Yu et al. (1996) for a mixture porosity ε of short ($L = 0.00391$ m) and

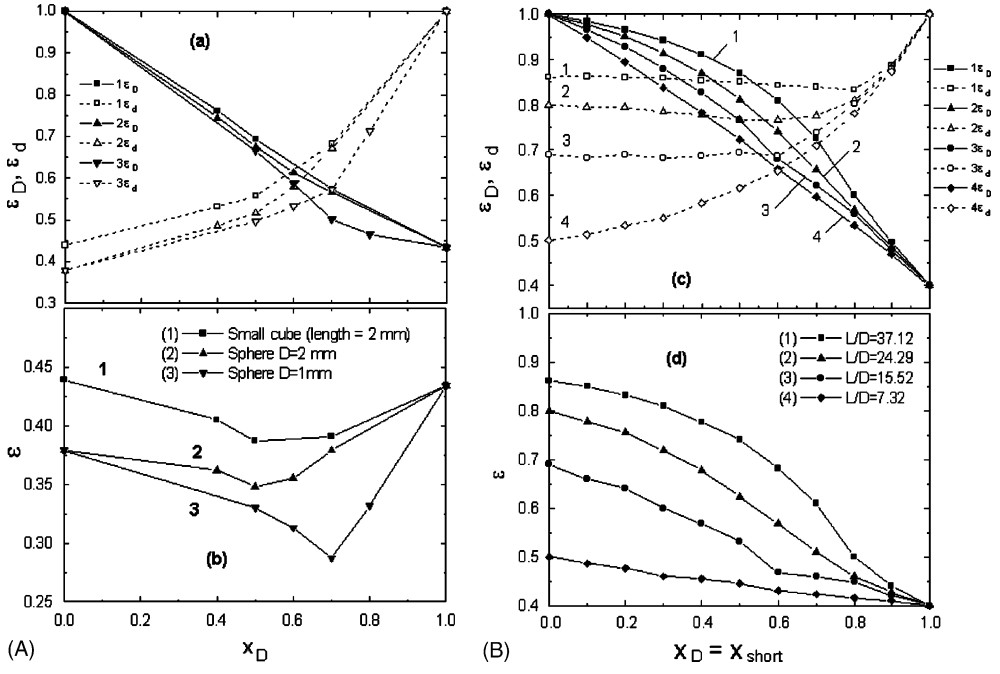

Fig. 9. Fractional porosities (a) and (b) overall porosity of mixture of cubes with cubes or spheres (A) (Yu et al., 1993) and (B) binary mixtures of short ($L = 0.00391$ m) and long cylinders of different L when the diameter for all cylinders $D = 0.00209$ m (Yu et al., 1996) vs. x_D. (A) Mixture of small and large cubes (1), and mixtures of large cubes with spheres (2)–(3), where x_D is the volume fraction of large cube (length 0.004 m). (B) The volume fraction of short cylinder was used here as $x_D = x_{\text{short}}$ by analogy with Yu et al. (1996); (a) and (c) fractional porosities; (b) and (d) overall porosity.

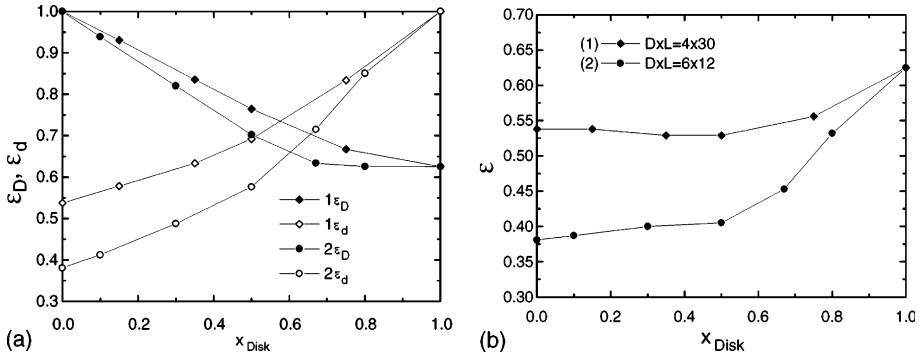

Fig. 10. Fractional porosities (a) and (b) overall porosity of the mixture of disks ($D = 0.019374$ and $L = 0.001384$ m) and cylinders of different $D \times L$ (Yu et al., 1993) vs. volume fraction of disks, x_{Disk}; ε_D and ε_d correspond to the fractional porosity of disk and cylinders, respectively.

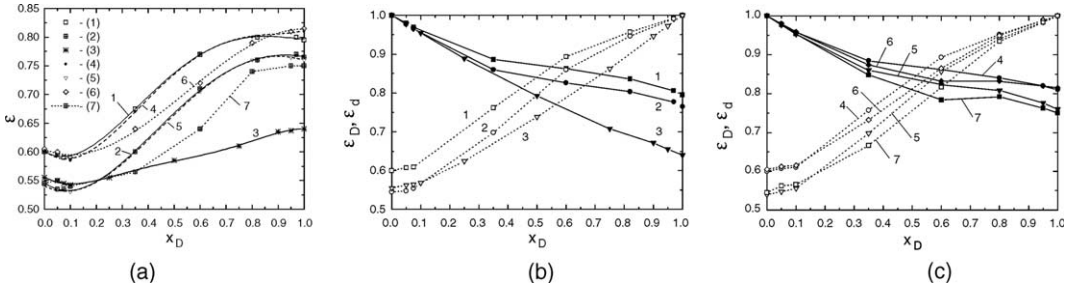

Fig. 11. Dependence of binary system porosity on volume fraction of large particles (filter aid): (a) overall porosity collected from Okoh (1989); (b) and (c) fractional porosity, where numbers correspond to enumeration in (a), LCR = liquefied coal residue. Curve 1—TiO_2 + perlite 416 (filtration pressure 76.5 kPa), curve 2—TiO_2 + perlite 416 (622 kPa), curve 3—$CaCO_3$ + talk (75.2 kPa), curve 4—LCR + celite 545 (75.2 kPa), curve 5—LCR + celite 545 (621 kPa), curve 6—LCR + celite 560 (76.5 kPa), curve 7—LCR + celite 545 (622 kPa). Celite 545 represents a coarse grade filter aid.

long cylinders with significant different length but equal cylinders (diameter $D = 0.00209$ m) (Fig. 9B). To keep the conditions reported in the work of Yu et al. (1996) we selected short cylinder particles as the governing fraction x_D and therefore $x_D = x_{short}$. At the same time the short cylinders are less irregular than long cylinders. With the increase in cylinder length their fractional porosity ε_d approaches the sphere + cylinder packing (Fig. 8).

A dependence of fractional porosity on volume fraction of disks x_{Disk} in a mixture of disks ($D = 0.0019374$ and $L = 0.001384$ m) and cylinders of different $D \times L$ (Yu et al., 1993) is shown in Fig. 10. All porosities are presented as a function of x_{Disk}. This means that ε_D and ε_d corresponds to the fractional porosity of disks and cylinders, respectively. As may be seen in Fig. 10, disk fraction plays a major role in overall porosity.

3.5.3. Cakes of large irregular and fine granular particles

The porosity and specific cake resistance as a function of the filter aid fraction were investigated by Okoh (1989). The following binary systems were used: small size particle fraction—liquefied coal residue (mineral matter and converted carbon), talc, calcium carbonate, titanium dioxide; filter aids diatomaceous earth and expanded perlite. Okoh showed that 10% or less of filter aid added to the suspension gives rise to a low porosity cake. The behaviour of the overall porosity is shown in Fig. 11.

When the size of granules corresponds to the fine fraction then, for the same size ratio D/d, the dependency curve of ε vs. x_D is a mirror-like image of Fig. 5 (see Fig. 11). However, the permeability vs. x_D behaves in the same way in both cases.

It seems then that when the particle size ratio D/d is large, less irregular (granular-like) particles are able to define the minimum porosity range around a volume fraction of 0.9–0.8, whereas irregular particles control the binary bed permeability whenever their volume fraction in the mixture is larger than 0.1–0.2.

4. Conclusion

It was found that the presence of more than 10% of fines in a coarse granular bed significantly reduces the cake porosity and hence the permeability. To improve cake permeability the volume fraction of filter aid in a suspension must be at least 50–60% of total solid volume.

The porosity behaviour can be analysed and predicted by means of the fractional porosity diagram. The minimal porosity of the mixture is a function of the size ratio between coarse and fine particles and can be estimated as a product of the different particles' bed porosities when small particles fill the void space left by the large particles skeleton. When we have kieselguhr as small size particles the overall porosity is constant from $x_D \sim 0.85$ up to $x_D = 1$. This means that a build up of a filter layer from a binary mixture is possible with a reduced consumption of kieselguhr.

It seems that the application of fractional porosities for binary mixture analysis (filter cake, sediments, column and catalyse pellet packing, etc.) may be a powerful tool to control the overall porosity and permeability by means of controlled changes in the properties of each particle fraction (particle shape, packing density, size ratio between and inside fractions, fractional content of the mixture).

It would also be interesting to simulate the evolution of dependencies of fractional porosities ε_D, ε_d and overall porosity ε on x_D in mass transfer processes such as dissolution (solid–liquid extraction) or growth of the particle fraction (crystallization). In such processes the fractional porosity and the overall porosity in a binary particle mixture are variable with time, hence, the permeability and diffusivity of a mixed bed is affected by the porosity variation. Extending the fractional porosity approach to the packing with changeable structure may give the additional possibility of developing effective methods for mass transfer control.

Acknowledgements

The authors thank FCT—Fundação para a Ciência e Tecnologia—for the grant given to Dr. Yelshin, as well for the funding the project on porous media, Ref POCTI/EQU/37500/2001, which made this work possible.

References

Abe, E., Hirosue, H., 1982. Porosity estimation of a mixed cake in body filtration. Journal of Chemical Engineering of Japan 15 (6), 490–493.

Brownell, L.E., Dombrovski, H.S., Dickey, C.A., 1950. Pressure drope through porous media. Part IV—new data and revised correlation. Chem. Eng. Progr. 46 (8), 415–422.

Klusácek, K., Schneider, P., 1981. Effect of size and shape of catalyst microparticles on pellet pore structure and effectiveness. Chem. Eng. Sci. 36 (3), 523–527.

Meeten, G.H., Sherwood, J.D., 1994. The hydraulic permeability of bentonite suspensions with granular inclusions. Chem. Eng. Sci. 49 (19), 3249–3256.

Mota, M., Teixeira, J.A., Bowen, R., Yelshin, A., 2000. Effect of tortuosity on transport properties of mixed granular beds. In: Proceedings of the 8th World Filtration Congress, 3–7 April 2000, vo1. 1. Filtration Society, Brighton, UK, pp. 57–60.

Mota, M., Teixeira, J.A., Yelshin, A., 1998. Tortuosity in bioseparations and its application to food processes. In: Feyo de Azevedo, Ferreira, E., Luben, K., Osseweijer, P. (Eds.), Proceedings of the 2nd European Symposium on Biochemical Engineering Science, Porto, 16–19 September 1998. University of Porto, Portugal, pp. 93–98.

Mota, M., Teixeira, J.A., Yelshin, A., 1999. Image analysis of packed beds of spherical particles of different sizes. Separation and Purification Technology 15, 59–68.

Mota, M., Teixeira, J.A., Yelshin, A., 2001. Binary spherical particle mixed beds porosity and permeability relationship measurement. Transactions of the Filtration Society 1 (4), 101–106.

Okoh, B.O., 1989. Porosity and permeability as a function of fraction of filter aid. Fluid/Particle Separation Journal 2 (1), 37–43.

Rushton, A., Ward, A.S., Holdich, R.G., 1996. Solid–Liquid Filtration and Separation Technology. VCH, Germany.

Tiller, F.M., Crump, J.R., Chen, W., Shen, Y.L., 1988a. Cycle optimization involving the use of filter aids. Particulate Science and Technology 6, 243–267.

Tiller, F.M., Crump, J.R., Chen, W., Shen, Y.L., 1988b. The effect of filter aids on cycle rates. In: Frederick, E.R., Mafrica, L.F. (Eds.), Anonymous Proceedings of the International Technical Conference on Filtration and Separation, Ocean City, Maryland, USA, 21–24 March 1988. AFS Kingwood, TX, pp. 471–478.

Weismantel, G., 2001. What's new in sewage sludge separation and processing? Filtration and Separation 38 (5), 22–25.

Weler, W.J., 1972. Physicochemical Processes for Water Quality Control. Wiley, USA, p. 182.

Yoon, S.-H., Murase, T., Iritani, E., 1992. Filtration with different kinds of diatomaceous precoating. Int. Chem. Eng. 32 (1), 172–180.

Yu, A.B., Standish, N., 1991. Estimation of the porosity of particle mixtures by a linear-mixture packing model. Ind. Eng. Chem. Res. 30 (6), 1372–1385.

Yu, A.B., Standish, N., 1993. A study of the packing of particles with a mixture size distribution. Powder Technology 76, 113–124.

Yu, A.B., Standish, N., McLean, A., 1993. Porosity calculation of binary mixtures of nonspherical particles. J. Am. Ceram. Soc. 76 (11), 2813–2816.

Yu, A.B., Zou, R.P., Standish, N., 1996. Modifying the linear packing model for predicting the porosity of nonspherical particle mixtures. Ind. Eng. Chem. Res. 35 (10), 3730–3741.